

Imido and Organometallic-Amido Titanium(IV) Complexes of a Chelating Phenanthrenediamide Ligand

Nicole A. Ketterer, Joseph W. Ziller, Arnold L. Rheingold, and Alan F. Heyduk*

Department of Chemistry, 1102 Natural Sciences 2, University of California, Irvine, California 92697 and the Department of Chemistry, University of California, San Diego, La Jolla, California 92093

Received February 6, 2007

New titanium(IV) complexes of the chelating ligand *N,N'*-bis(3,5-dimethylphenyl)-phenanthrene-9,10-diamide (pada²⁻) are described. Metalation of padaH₂ with TiCl₄ in the presence of base afforded the six-coordinate pyridine adduct (pada)TiCl₂(py)₂ (**1**), which was used as a starting point for all further complexes presented in this work. Metathesis of **1** with LiN(SiMe₃)₂ afforded the four-coordinate complex (pada)TiCl[N(SiMe₃)₂] (**2**), free of coordinating pyridine. Further elaboration of **2** with MeLi, PhLi, and PhCH₂MgCl provided the mixed alkyl-amido species (pada)TiR[N(SiMe₃)₂] (**3a**, R = Me; **3b**, R = CH₂Ph; **3c**, R = Ph), which are all stable in the solid state and in solution. Dichloride **1** reacts directly with 2 equiv of PhCH₂MgCl to give the five-coordinate complex (pada)Ti(CH₂Ph)₂(py) (**4**). The corresponding dimethyl- and diphenyltitanium complexes could not be isolated; however, generation of these species followed by in situ reaction with ^tBuNH₂ afforded the new titanium imido complex (pada)-Ti(=N^tBu)(py)₂ (**6**). The aryl imido derivative (pada)Ti(=N(2,6-C₆H₃Me₂))(py)₂ (**7**) was prepared by transimination of **6** with 2,6-dimethylaniline. Imido complex **6** also reacted with benzaldehyde to give the organic metathesis product benzadimine; however, more crowded ketone and imine substrates were unreactive. Prolonged heating of **6** in the absence of reactive substrates led to irreversible dimerization, forming [(pada)Ti(py)(μ-N^tBu)]₂ (**8**).

Introduction

Imido and organometallic-amido complexes of titanium are of interest for a variety of catalytic and stoichiometric nitrogen-group transfer reactions. Alkene and alkyne hydroamination,^{1–17} olefin polymerization,^{18–22} imine metathesis,^{23–26} and C–H

bond activation strategies^{27–29} have been devised to capitalize on the reactive nature of Ti–C, Ti–N, and Ti=N bonds. Mechanistic studies of alkene and alkyne hydroamination suggest that the reactive intermediate is a Group IV imido species generated from a bisamide metal precursor.³⁰ While titanium alkyl and amide complexes show enhanced hydroamination reactivity,⁴ complexes with chelating η¹-pyrrole-based ligands have been found to be even more reactive thanks to increased Lewis acidity at the titanium center.^{5,31} In imine metathesis reactions steric and electronic parameters on both the imine moiety as well as the imido group have a measurable

* To whom correspondence should be addressed. E-mail: aheyduk@uci.edu.

(1) Ackermann, L.; Bergman, R. G.; Loy, R. N. *J. Am. Chem. Soc.* **2003**, *125*, 11956–11963.

(2) Tillack, A.; Castro, I. G.; Hartung, C. G.; Beller, M. *Angew. Chem., Int. Ed.* **2002**, *41*, 2541–2543.

(3) Ong, T. G.; Yap, G. P. A.; Richeson, D. S. *Organometallics* **2002**, *21*, 2839–2841.

(4) Haak, E.; Bytschkov, I.; Doye, S. *Angew. Chem., Int. Ed.* **1999**, *38*, 3389–3391.

(5) Shi, Y.; Ciszewski, J. T.; Odom, A. L. *Organometallics* **2001**, *20*, 3967–3969.

(6) Johnson, J. S.; Bergman, R. G. *J. Am. Chem. Soc.* **2001**, *123*, 2923–2924.

(7) Ayinla, R. O.; Schafer, L. L. *Inorg. Chim. Acta* **2006**, *359*, 3097–3102.

(8) Kaspar, L. T.; Fingerhut, B.; Ackermann, L. *Angew. Chem., Int. Ed.* **2005**, *44*, 5972–5974.

(9) Bexrud, J. A.; Beard, J. D.; Leitch, D. C.; Schafer, L. L. *Org. Lett.* **2005**, *7*, 1959–1962.

(10) Ackermann, L.; Bergman, R. G. *Org. Lett.* **2002**, *4*, 1475–1478.

(11) Tillack, A.; Khedkar, V.; Beller, M. *Tetrahedron Lett.* **2004**, *45*, 8875–8878.

(12) Esteruelas, M. A.; Lopez, A. M.; Mateo, A. C.; Onate, E. *Organometallics* **2006**, *25*, 1448–1460.

(13) Buil, M. L.; Esteruelas, M. A.; Lopez, A. M.; Mateo, A. C. *Organometallics* **2006**, *25*, 4079–4089.

(14) Muller, C.; Loos, C.; Schulenberg, N.; Doye, S. *Eur. J. Org. Chem.* **2006**, 2499–2503.

(15) Takaki, K.; Koizumi, S.; Yamamoto, Y.; Komeyama, K. *Tetrahedron Lett.* **2006**, *47*, 7335–7337.

(16) Zhang, Z.; Leitch, D. C.; Lu, M.; Patrick, B. O.; Schafer, L. L. *Chem. Eur. J.* **2007**, *13*, 2012–2022.

(17) Hoover, J. M.; Petersen, J. R.; Pikul, J. H.; Johnson, A. R. *Organometallics* **2004**, *23*, 4614–4620.

(18) Adams, N.; Arts, H. J.; Bolton, P. D.; Cowell, D.; Dubberley, S. R.; Friederichs, N.; Grant, C. M.; Kranenburg, M.; Sealey, A. J.; Wang, B.; Wilson, P. J.; Zuideveld, M.; Blake, A. J.; Schroder, M.; Mountford, P. *Organometallics* **2006**, *25*, 3888–3903.

(19) Bigmore, H. R.; Dubberley, S. R.; Kranenburg, M.; Lawrence, S. C.; Sealey, A. J.; Selby, J. D.; Zuideveld, M. A.; Cowley, A. R.; Mountford, P. *Chem. Commun.* **2006**, 436–438.

(20) Groysman, S.; Tshuva, E. Y.; Goldberg, I.; Kol, M.; Goldschmidt, Z.; Shuster, M. *Organometallics* **2004**, *23*, 5291–5299.

(21) Scollard, J. D.; McConville, D. H. *J. Am. Chem. Soc.* **1996**, *118*, 10008–10009.

(22) Taberero, V.; Cuenca, T. *Eur. J. Inorg. Chem.* **2005**, 338–346.

(23) McInnes, J. M.; Blake, A. J.; Mountford, P. *J. Chem. Soc., Dalton Trans.* **1998**, 3623–3628.

(24) McInnes, J. M.; Mountford, P. *Chem. Commun.* **1998**, 1669–1670.

(25) Wang, H.; Chan, H.; Xie, Z. *Organometallics* **2005**, *24*, 3772–3779.

(26) Guiducci, A. E.; Boyd, C. L.; Mountford, P. *Organometallics* **2006**, *25*, 1167–1187.

(27) Bashall, A.; Collier, P. E.; Gade, L. H.; McPartlin, M.; Mountford, P.; Trosch, D. J. M. *Chem. Commun.* **1998**, 2555–2556.

(28) Bennett, J. L.; Wolczanski, P. T. *J. Am. Chem. Soc.* **1994**, *116*, 2179–2180.

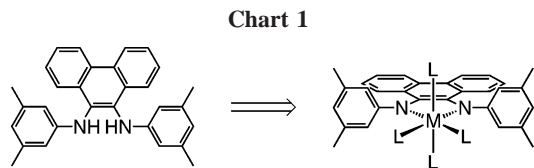
(29) Polse, J. L.; Andersen, R. A.; Bergman, R. G. *J. Am. Chem. Soc.* **1998**, *120*, 13405–13414.

(30) Walsh, P. J.; Baranger, A. M.; Bergman, R. G. *J. Am. Chem. Soc.* **1992**, *114*, 1708–1719.

(31) Odom, A. L. *Dalton* **2005**, 225–233.

impact on reaction rates.²⁴ C–H bond activations are perhaps most sensitive to the titanium coordination environment. Access to electronically and coordinatively unsaturated, three-coordinate, titanium–imido complexes leads to facile activation of the most robust C–H bonds by a 1,2-addition pathway; however, addition of a fourth donor ligand stabilizes the titanium–imido functionality, shutting down the C–H bond activation chemistry completely.^{28,29,32}

Synthetic efforts have focused on the preparation of titanium complexes supported by new auxiliary ligands that control the steric and electronic parameters governing reactivity at the titanium metal center. While the soft coordination environment of Cp-type ligands has permitted the synthesis of a variety of titanium–imido and –amido complexes,^{33–41} the potential reactivity of complexes supported by hard π -donor ligands has made modular, sterically demanding nitrogen-donor ligands attractive. Ligands with hard donor atoms such as N, O, and Cl form strong M–L bonds to titanium^{42,43} and allowed the synthesis of imido and organometallic–amido titanium complexes.^{44–56} For example, titanium–imido complexes with chelating amidinate ligands exhibit a range of insertion reactivity with unsaturated substrates such as carbodiimides, CO₂, COS, and isocyanates.^{3,26,57,58} Likewise, titanium centers with chelating



β -diketiminato ligands support many metal–ligand multiple-bond structures including imidos,^{55–57,59,60} alkylidenes,^{61–63} and phosphinidenes.^{63–65} In these cases, the monoanionic, chelating nitrogen ligand provides both strong electron donation and steric protection to the electrophilic titanium center.

N,N'-Bis(aryl)phenanthrenediamine-derived ligands, shown in Chart 1, are an attractive platform for studying the reactivity of titanium imido and organometallic–amido complexes. In its deprotonated form an *N,N'*-bis(aryl)phenanthrenediamide ligand has two anionic π -donor nitrogen atoms, yet π donation is moderated by conjugation of the nitrogen lone pair into the phenanthrene ring system. The aromaticity of this ring system also can protect the ligand backbone against the degradation pathways observed for other unsaturated chelating ligands such as β -diketiminato.^{62,66} A limited bite angle is enforced by the rigid planarity of the phenanthrene ring system, providing a uniform metal template for reactivity studies. Finally, steric protection for the metal center can be installed via substituents on the amide nitrogen donors, thus regulating access to the metal center. Herein we report on the titanium coordination chemistry of *N,N'*-bis(3,5-dimethylphenyl)phenanthrene-9,10-diamide (pada²⁻), including the synthesis and characterization of the first imido and organometallic–amido complexes of a phenanthrenediamide ligand.

Results and Discussion

Synthesis and Metalation of padaH₂. Transition-metal complexes derived from 9,10-phenanthrenediamine are known;^{67–69} yet the chemistry of *N*-aryl-substituted derivatives is underdeveloped, perhaps for lack of an efficient ligand synthesis. Scheme 1 shows our strategy for the preparation of *N,N'*-bis(3,5-dimethylphenyl)phenanthrene-9,10-diamine (padaH₂) via reductive cyclodehydrogenation of 1,2-bis(3,5-dimethylphenylimino)-1,2-diphenylethane. Previous reports used lithium metal and extended reaction times to achieve such cyclization reactions;^{70–72} in our experience, K₂C₈ produces good yields of

(32) Cummins, C. C.; Schaller, C. P.; Van Duyne, G. D.; Wolczanski, P. T.; Chan, A. W. E.; Hoffmann, R. J. *Am. Chem. Soc.* **1991**, *113*, 2985–2994.

(33) Dunn, S. C.; Hazari, N.; Cowley, A. R.; Green, J. C.; Mountford, P. *Organometallics* **2006**, *25*, 1755–1770.

(34) Ciruelos, S.; Cuenca, T.; Gomez, R.; Gomez-Sal, P.; Manzanero, A.; Royo, P. *Organometallics* **1996**, *15*, 5577–5585.

(35) Kissoukko, D. A.; Guzei, I. A.; Gellman, S. H.; Stahl, S. S. *Organometallics* **2005**, *24*, 5208–5210.

(36) Kunz, K.; Erker, G.; Doring, S.; Frohlich, R.; Kehr, G. *J. Am. Chem. Soc.* **2001**, *123*, 6181–6182.

(37) Jin, J.; Chen, E. Y. *Organometallics* **2002**, *21*, 13–15.

(38) Hanna, T. E.; Keresztes, I.; Lobkovsky, E.; Bernskoetter, W. H.; Chirik, P. J. *Organometallics* **2004**, *23*, 3448–3458.

(39) Owen, C. T.; Bolton, P. D.; Cowley, A. R.; Mountford, P. *Organometallics* **2007**, *26*, 83–92.

(40) Bai, Y.; Roesky, W. H.; Noltmeyer, M. Z. *Anorg. Allg. Chem.* **1991**, *595*, 21–26.

(41) Martins, A. M.; Ascenso, J. R.; Azevedo, C. G.; Calhorda, M. J.; Dias, A. R.; Rodrigues, S. S.; Toupet, L.; Leonardis, P.; Veiros, L. F. *J. Chem. Soc., Dalton Trans.* **2000**, 4332–4338.

(42) Wilkinson, G.; Stone, F. G. A.; Abel, E. W. *Comprehensive Organometallic Chemistry*; Pergamon: Oxford, 1982; Vol. 3.

(43) Cotton, F. A.; Wilkinson, G.; Murillo, C. A.; Bochmann, M. *Advanced Inorganic Chemistry*, 6th ed.; Wiley: New York, 1999.

(44) Manzer, L. E. *J. Am. Chem. Soc.* **1977**, *99*, 276–277.

(45) Yelamos, C.; Heeg, M. J.; Winter, C. H. *Organometallics* **1999**, *18*, 1168–1176.

(46) Adams, N.; Arts, H. J.; Bolton, P. D.; Cowell, D.; Dubberley, S. R.; Friederichs, N.; Grant, C. M.; Kranenburg, M.; Sealey, A. J.; Wang, B.; Wilson, P. J.; Zuideveld, M.; Blake, A. J.; Schroder, M.; Mountford, P. *Organometallics* **2006**, *25*, 3888–3903.

(47) Carmalt, C. J.; Newport, A. C.; O'Neill, S. A.; Parkin, I. P.; White, A. J. P.; Williams, D. J. *Inorg. Chem.* **2005**, *44*, 615–619.

(48) Skinner, M. E. G.; Toupance, T.; Cowhig, D. A.; Tyrrell, B. R.; Mountford, P. *Organometallics* **2005**, *24*, 5586–5603.

(49) Irigoyen, A. M.; Martin, A.; Mena, M.; Palacios, F.; Yelamos, C. *J. Organomet. Chem.* **1995**, *494*, 255–259.

(50) Li, Y.; Shi, Y.; Odom, A. L. *J. Am. Chem. Soc.* **2004**, *126*, 1794–1803.

(51) Stewart, P. J.; Blake, A. J.; Mountford, P. *Organometallics* **1998**, *17*, 3271–3281.

(52) Bolton, P. D.; Adams, N.; Clot, E.; Cowley, A. R.; Wilson, P. J.; Schroder, M.; Mountford, P. *Organometallics* **2006**, *25*, 5549–5565.

(53) Pietryga, J. M.; Jones, J. N.; Macdonald, C. L. B.; Moore, J. A.; Cowley, A. H. *Polyhedron* **2006**, *25*, 259–265.

(54) Mountford, P. *Chem. Commun.* **1997**, 2127–2134.

(55) Croft, A.; Charis, R.; Boyd, C. L.; Cowley, A. R.; Mountford, P. *J. Organomet. Chem.* **2003**, *683*, 120–130.

(56) Bailey, B. C.; Basuli, F.; Huffman, J. C.; Mindiola, D. J. *Organometallics* **2006**, *25*, 2725–2728.

(57) Ong, T. G.; Yap, G. P. A.; Richeson, D. S. *J. Am. Chem. Soc.* **2003**, *125*, 8100–8101.

(58) Guiducci, A. E.; Cowley, A. R.; Skinner, M. E. G.; Mountford, P. *J. Chem. Soc., Dalton Trans.* **2001**, 1392–1394.

(59) Hazari, N.; Mountford, P. *Acc. Chem. Res.* **2005**, *38*, 839–849.

(60) Basuli, F.; Huffman, J. C.; Mindiola, D. J. *Inorg. Chem.* **2003**, *42*, 8003–8010.

(61) Basuli, F.; Bailey, B. C.; Huffman, J. C.; Mindiola, D. J. *Chem. Commun.* **2003**, 1554–1555.

(62) Basuli, F.; Bailey, B. C.; Huffman, J. C.; Mindiola, D. J. *Organometallics* **2005**, *24*, 3321–3334.

(63) Mindiola, D. J. *Acc. Chem. Res.* **2006**, *39*, 813–821.

(64) Zhao, G.; Basuli, F.; Kilgore, U. J.; Fan, H.; Aneetha, H.; Huffman, J. C.; Wu, G.; Mindiola, D. J. *J. Am. Chem. Soc.* **2006**, *128*, 13575–13585.

(65) Basuli, F.; Tomaszewski, J.; Huffman, J. C.; Mindiola, D. J. *J. Am. Chem. Soc.* **2003**, *125*, 10170–10171.

(66) Basuli, F.; Bailey, B. C.; Watson, L. A.; Tomaszewski, J.; Huffman, J. C.; Mindiola, D. J. *Organometallics* **2005**, *24*, 1886–1906.

(67) vanBelzen, R.; Hoffmann, H.; Elsevier, C. J. *Angew. Chem., Int. Ed.* **1997**, *36*, 1743–1745.

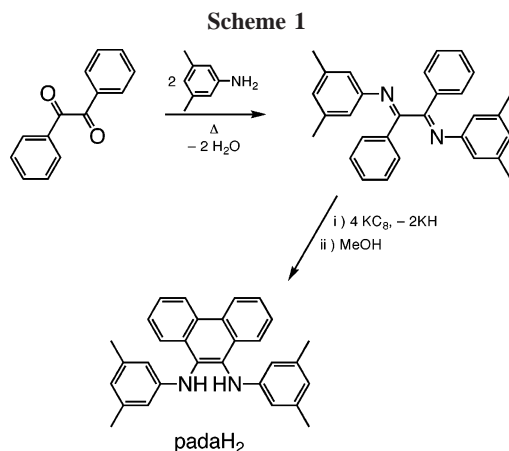
(68) Andoseh, I. N.; Douglas, I.; Egharevba, G. O.; Megnamisi-Belombe, M. Z. *Z. Anorg. Allg. Chem.* **1982**, *484*, 203–209.

(69) vanBelzen, R.; Klein, R. A.; Kooijman, H.; Veldman, N.; Spek, A. L.; Elsevier, C. J. *Organometallics* **1998**, *17*, 1812–1825.

(70) Macpherson, E. J.; Smith, J. G. *Tetrahedron* **1971**, *27*, 2645–2649.

(71) MacPherson, E. J.; Smith, J. G. *Chem. Commun.* **1970**, 1552–1553.

(72) vanBelzen, R.; Klein, R. A.; Smeets, W. J. J.; Spek, A. L.; Benedix, R.; Elsevier, C. J. *Recl. Trav. Chim. Pays-Bas* **1996**, *275*–285.



the desired phenanthrenediamine product under milder conditions. Eight resonances are observed in the ¹H NMR spectrum of padaH₂: four aryl resonances at 7.31, 7.38, 8.20, and 8.52 ppm, displaying the proper coupling patterns, are observed for the phenanthrene backbone, while the 3,5-dimethylphenyl substituents give rise to singlets at 1.97, 6.23, and 6.39 ppm. The N–H resonance of the neutral diamine is visible as a sharp singlet at 5.5 ppm in C₆D₆.

The six-coordinate metal complex, (pada)TiCl₂(py)₂ (**1**), was prepared in 96% yield by direct addition of padaH₂ to TiCl₄ in the presence of base. Well-formed single crystals were obtained from slow diffusion of pentane into a dichloromethane solution of **1**; however, crystals grown in this manner readily lose solvent, resulting in poor-quality X-ray diffraction data. The molecular connectivity of **1** shown in Figure 1 was obtained repeatedly from data sets acquired using several different crystals. The titanium coordination environment in **1** is pseudo-octahedral, with nominal C_{2v} symmetry. The two chloride ions occupy trans positions with two cis pyridine ligands and the chelating pada²⁻ ligand adopting a puckered and bent conformation. Similar distortions in metal complexes with unsaturated diamide ligands have been attributed to an η⁴ interaction that allows donation of the C=C π electrons of the ligand into an empty metal d_{z²} orbital.^{73–78} An alternative explanation, supported by recent experimental and theoretical studies of d⁰ molybdenum and tungsten complexes, suggests that this structural distortion serves to increase π overlap between the nitrogen lone electron pairs and the empty metal d_{xy} orbital of the titanium center.^{79–81} In the case of **1**, the latter bonding model is supported by the molecular structure. The six-coordinate geometry of **1** means the d_{z²} orbital is strongly antibonding, which decreases its ability to participate in π bonding. Furthermore, the sum of angles around each nitrogen atom of the pada²⁻ ligand is consistent

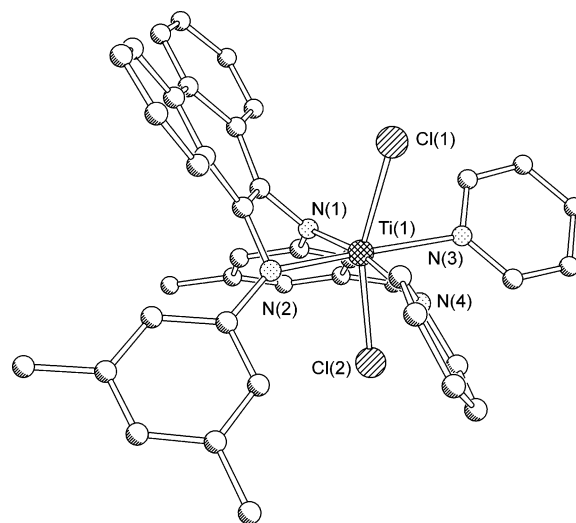
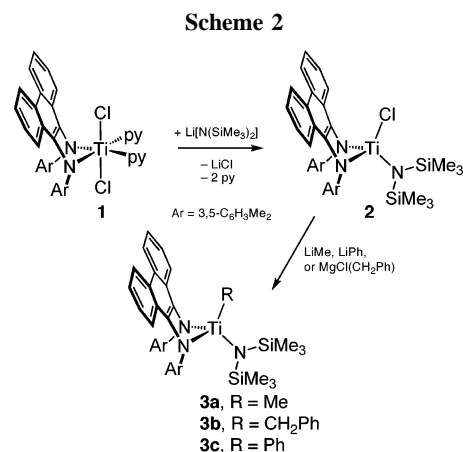


Figure 1. Molecular structure of (pada)TiCl₂(py)₂ (**1**) as determined by X-ray diffraction. Hydrogen atoms and the solvent molecule are omitted for clarity.



with sp² hybridization. The nodal plane of these amide donors is rotated by 48° relative to the equatorial plane of the titanium center, which increases overlap between the amide lone electron pair and the empty titanium d_{xy} orbital.

The solution ¹H NMR spectrum of **1** is consistent with the solid-state structure, though broadened resonances suggest a fluxional coordination environment. Upon cooling the sample to 275 K, all proton resonances sharpened and no new peaks were observed. The ¹H NMR spectrum with added pyridine displayed separate resonances for free and coordinated pyridine, indicating that pyridine dissociation from **1** is slow on the NMR time scale.

Synthesis of Organometallic–Amido Titanium Complexes. Complex **1** reacted readily with the lithium amide reagent LiN(SiMe₃)₂ to afford (pada)TiCl[N(SiMe₃)₂] (**2**) as shown in Scheme 2. Recrystallization of **2** from pentane at –35 °C gave medium-red blocks suitable for X-ray diffraction. The molecular structure of **2** is shown in Figure 2, and selected bond lengths and angles are shown in Table 1. The packing diagram for **2** suggests an intermolecular π-stacked arrangement with a long centroid–centroid distance of ~3.6 Å (see Supporting Information).⁸² The coordination environment about the titanium center is distorted tetrahedral with a Cl(1)–Ti(1)–N(3) bond angle of 114.50(5)° and ligand bite angle of 87.65(6)°. The Ti–

(73) Pindado, G. J.; Thornton-Pett, M.; Bochmann, M. *J. Chem. Soc., Dalton Trans.* **1998**, 393–400.

(74) Tom Dieck, H.; Rieger, H. J.; Fendesak, G. *Inorg. Chim. Acta* **1990**, *177*, 191–197.

(75) Scholz, J.; Hadi, G. A.; Thiele, K.; Gors, H.; Weimann, R.; Schumann, H.; Sieler, J. *J. Organomet. Chem.* **2001**, *626*, 243–259.

(76) Chamberlain, L. R.; Durfee, L. D.; Fanwick, P. E.; Kobriger, L. M.; Latesky, S. L.; McMullen, A. K.; Steffey, B. D.; Rothwell, I. P.; Foltin, K.; Huffman, J. C. *J. Am. Chem. Soc.* **1987**, *109*, 6068–6076.

(77) Scholz, J.; Dlikan, M.; Strohl, D.; Dietrich, A.; Schuman, H.; Thiele, K. *Chem. Ber.* **1990**, *123*, 2279–2285.

(78) Aoyagi, K.; Gantzel, P.; Kalai, K.; Tilley, T. D. *Organometallics* **1996**, *15*, 923–927.

(79) Ison, E. A.; Cameron, T. M.; Abboud, K. A.; Boncella, J. M. *Organometallics* **2004**, *23*, 4070–4076.

(80) Galindo, A.; Ienco, A.; Mealli, C. *Comm. Inorg. Chem.* **2002**, *23*, 401–416.

(81) Wang, S. S.; Abboud, K. A.; Boncella, J. M. *J. Am. Chem. Soc.* **1997**, *119*, 11990–11991.

(82) Bu, X. H.; Tong, M. L.; Xie, Y. B.; Li, J. R.; Chang, H. C.; Kitagawa, S.; Ribas, J. *Inorg. Chem.* **2005**, *44*, 9837–9846.

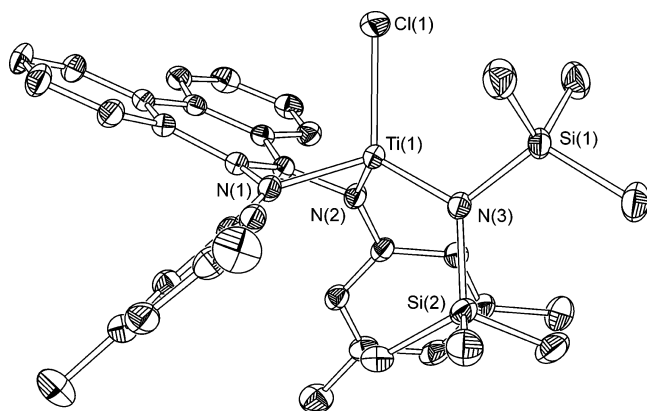


Figure 2. Thermal ellipsoid plot of (pada)TiCl[N(SiMe₃)₂]·C₆H₆ (2·C₆H₆). Ellipsoids are shown at 50% probability, while hydrogen atoms and the solvent molecule have been omitted for clarity.

Table 1. Selected Bond Lengths (Å) and Angles (deg) for (pada)TiCl[N(SiMe₃)₂]·C₆H₆ (2·C₆H₆)

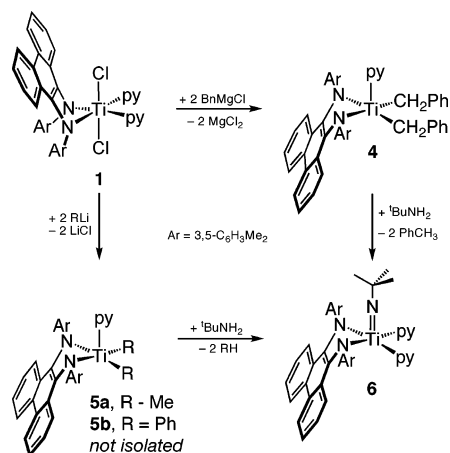
bond lengths		bond angles	
Ti(1)–N(1)	1.9131(15)	Cl(1)–Ti(1)–N(1)	106.43(5)
Ti(1)–N(2)	1.9033(15)	Cl(1)–Ti(1)–N(2)	113.42(5)
Ti(1)–N(3)	1.8905(15)	Cl(1)–Ti(1)–N(3)	114.50(5)
Ti(1)–Cl(1)	2.2686(6)	N(1)–Ti(1)–N(2)	87.65(6)

(1)–N(3) and Ti(1)–Cl(1) bond lengths are 1.8905(15) and 2.2686(6) Å, respectively. The Si(1)–N(3)–Ti(1)–Cl(1) torsion angle of ~5° forces one Me₃Si group of the amide ligand to be in close proximity to the chloride (~3.72 Å).

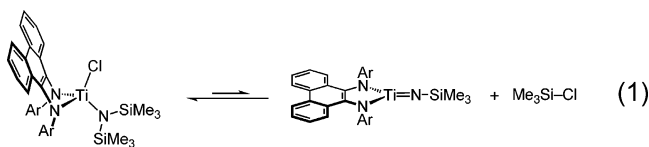
In solution, the room-temperature ¹H NMR spectrum of **2** showed broad signals indicative of a coordination environment that is fluxional on the NMR time scale. At 298 K, one broad resonance was observed at 0.13 ppm for both trimethylsilyl groups of the monodentate amide ligand. Similarly, a single broad resonance at 2.26 ppm was observed for the four methyl groups of the phenanthrenediamide ligand. Variable-temperature ¹H NMR studies were used to investigate the fluxional processes giving rise to the observed line broadening. Upon cooling the sample to 238 K, the broad trimethylsilyl resonance at 2.26 ppm splits into sharp singlets at 2.40 and 2.03 ppm. Similarly, the broad methyl resonance at 0.13 ppm splits into sharp singlets at –0.29 and 0.56 ppm. The exchange process was modeled using the complete band shape method⁸³ to afford rate constants between 238 and 313 K; an Eyring analysis (see Supporting Information) provided the activation parameters $\Delta H^\ddagger = 23 \pm 2$ kcal mol^{–1} and $S^\ddagger = 31 \pm 5$ eu.

Thermolysis of **2** was carried out in an attempt to eliminate Me₃SiCl and form a three-coordinate imido species (eq 1). The orientation of the chloride and amide ligands in the solid-state structure of **2** suggested that Me₃SiCl elimination may be possible. A similar Si–N–Ti–Cl arrangement was reported for (nacnac)Ti^{III}Cl[N(SiMe₃)₂], which upon one-electron oxidation eliminated Me₃SiCl to form a titanium(IV) imido complex.⁵⁶ The high activation enthalpy and large and positive activation entropy measured for **2** are consistent with a dissociative process, suggesting that Me₃SiCl elimination may be operative at room temperature. Heating benzene-*d*₆ solutions of **2** to 140 °C resulted in no change over 48 h. Similarly, thermolysis reactions carried out in the presence of diphenylacetylene or benzophenone to trap the putative three-coordinate imido showed no change after 12 h. These results suggest that if Me₃–

Scheme 3



SiCl extrusion occurs as shown in eq 1, the reverse 1,2-addition reaction must be much faster than any other unimolecular or bimolecular process to trap the putative three-coordinate imido fragment.



Organometallic derivatives of **2** were prepared by metathesis with the appropriate Grignard or organolithium reagents (Scheme 2). Methyl-, benzyl-, and phenylamide complexes **3a–c** were prepared in 73–94% yield, and all species were isolated as red-orange amorphous solids. The distinguishing ¹H NMR features for **3a–c** correspond to the hydrocarbon ligands. The ¹H NMR spectrum of methyl derivative **3a** showed a singlet at 0.44 ppm, while the benzylic protons of **3b** were observed as a singlet at 2.35 ppm. Derivative **3c** showed three aryl resonances for the phenyl ligand, suggesting that rotation about the Ti–C bond is fast in room-temperature solution. Other ¹H NMR markers for **3a–c** were diagnostic for the titanium-coordinated pada^{2–} ligand.

Synthesis and Characterization of Bis(benzyl)titanium and Imidotitanium Complexes. The bis(benzyl)titanium complex (pada)Ti(CH₂Ph)₂(py) (**4**) was obtained by reaction of benzyl Grignard with **1**. While **4** was formed in high yields, it was always contaminated with up to 20% bibenzyl.⁸⁴ Recrystallization from pentane at –35 °C afforded higher purity material, but the yield of **4** was reduced significantly. The ¹H NMR spectrum of **4** suggested that one pyridine molecule is coordinated to the titanium center, but pyridine dissociation occurs readily to form a four-coordinate species, (pada)Ti(CH₂Ph)₂. The room-temperature ¹H NMR spectrum of **4** with one added equivalent of pyridine showed only one set of pyridine resonances, consistent with fast exchange between free and coordinated pyridine on the NMR time scale. The ¹H NMR resonances for the pada^{2–} ligand and the two benzyl moieties are symmetric, also consistent with rapid pyridine exchange via a four-coordinate (pada)Ti(CH₂Ph)₂ intermediate.

Attempts to isolate dimethyl- or diphenyltitanium(IV) complexes analogous to **4** were unsuccessful; however, these putative species can be made and used in situ to prepare new titanium imido complexes. Addition of MeLi or PhLi to **1** at low

(83) Sandstrom, J. *Dynamic NMR Spectroscopy*; Academic Press, Inc.: New York, 1982.

(84) Axenov, K. V.; Kilpelainen, I.; Klinga, M.; Leskela, M.; Repo, T. *Organometallics* **2006**, *25*, 463–471.

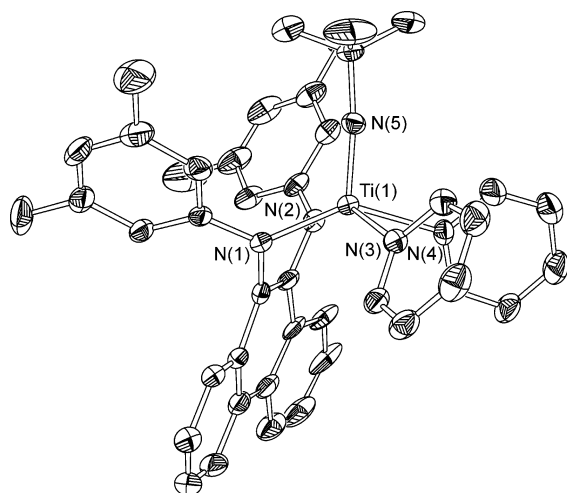


Figure 3. Thermal ellipsoid plot of (pada)Ti(=N^tBu)(py)₂·OEt₂ (**6**·OEt₂). Ellipsoids are shown at 50% probability, while hydrogen atoms and the solvent molecule have been omitted for clarity.

Table 2. Selected Bond Lengths (Å) and Angles (deg) for (pada)Ti(=N^tBu)(py)₂·OEt₂ (6**·OEt₂)**

bond lengths		bond angles	
Ti(1)–N(1)	2.012(3)	N(5)–Ti(1)–N(1)	112.49(14)
Ti(1)–N(2)	2.013(3)	N(5)–Ti(1)–N(2)	110.39(14)
Ti(1)–N(3)	2.252(3)	N(5)–Ti(1)–N(3)	97.92(13)
Ti(1)–N(4)	2.233(3)	N(5)–Ti(1)–N(4)	104.80(14)
Ti(1)–N(5)	1.699(3)	N(1)–Ti(1)–N(2)	82.63(13)
		Ti(1)–N(5)–C(41)	173.6(3)

temperature resulted in precipitation of LiCl as a white solid and development of a dark red solution, as observed during the synthesis of bis(benzyl) derivative **4**. While neither of these putative complexes (pada)TiMe₂(py) (**5a**) or (pada)TiPh₂(py) (**5b**) could be isolated, addition of *tert*-butylamine to cold solutions of **5a** or **5b** resulted in formation of (pada)Ti(=N^tBu)(py)₂ (**6**), as shown in Scheme 3. In this way, the new imido complex **6** was prepared in 53% yield. Similarly, pure samples of **4** treated with *tert*-butylamine formed **6** and two equivalents of toluene.

X-ray diffraction studies of imido complex **6** revealed a square pyramidal titanium center with an apical imido ligand. Yellow crystals of **6** were obtained from diethyl ether at –35 °C; the solid-state molecular structure of **6** is shown as a thermal ellipsoid plot in Figure 3, and selected bond lengths and angles are presented in Table 2. Five-coordinate titanium imido complexes with apical imido ligands are well established, and the stability of this structural motif has been attributed to the strong trans effect of the imido ligand.^{85,86} The five-coordinate geometry of **6** stands in contrast to related imidotitanium complexes supported by neutral α -diimine ligands, which adopt six-coordinate geometries.²³ The apical imide ligand of **6** also has a short Ti–N bond length (1.699(3) Å) relative to imido complexes supported by α -diimine ligands (Ti–N 1.729(4) Å). This short bond distance is consistent with a formal triple bond between the N and Ti atoms,^{86–90} and this assignment is further supported by a nearly linear Ti–N–C bond angle (173.6(3)°).

(85) Blake, A. J.; Collier, P. E.; Unn, S. C.; Li, W.; Mountford, P.; Shishkin, O. V. *J. Chem. Soc., Dalton Trans.* **1997**, 1549–1558.

(86) Kaltsoyannis, N.; Mountford, P. *J. Chem. Soc., Dalton Trans.* **1999**, 781–789.

(87) Lewkebandara, T. S.; Sheridan, P. H.; Heeg, M. J.; Rheingold, A. L.; Winter, C. H. *Inorg. Chem.* **1994**, *33*, 5879–5889.

(88) Parsons, T. B.; Hazari, N.; Cowley, A. R.; Green, J. C.; Mountford, P. *Inorg. Chem.* **2005**, *44*, 8442–8458.

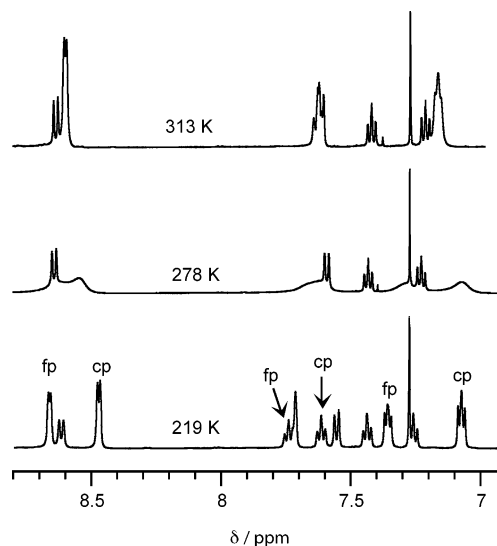


Figure 4. Variable-temperature ¹H NMR spectra (500 MHz, CDCl₃) for (pada)Ti(=N^tBu)(py)₂ (**6**) in the presence of 2 equiv of free pyridine (fp = free pyridine, cp = coordinated pyridine).

Simple symmetry arguments dictate that both nitrogen lone pairs can donate into empty titanium d_{xz} and d_{yz} orbitals to form the Ti≡N triple bond. The basal plane of **6** is occupied by two pyridine molecules and the pada²⁻ ligand. The N(1)–Ti(1)–N(2) bite angle is again small at 82.63(13)°, and the phenanthrene ring is bent away from the apical imido ligand and toward the open coordination site of the Ti center.^{55,85} As observed for **1**, the amide donors of the pada²⁻ ligand in **6** are rotated to maximize overlap between the filled amide p_z orbital and the empty titanium d_{xy} orbital.

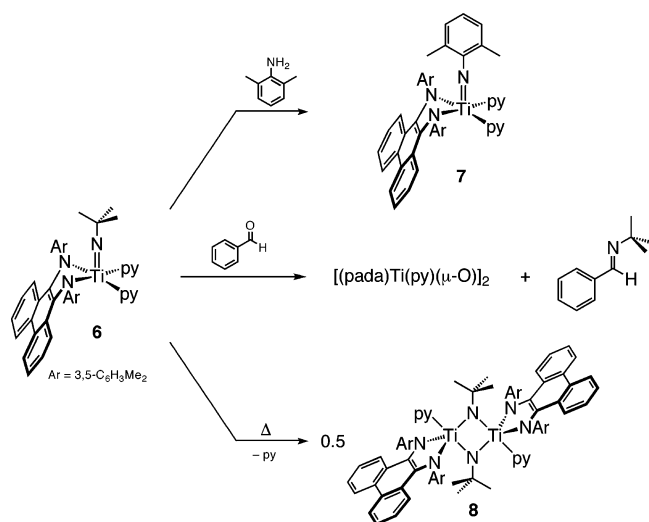
In solution, the five-coordinate titanium imido complex **6** undergoes fast, dissociative pyridine exchange. At 298 K, three exchange-broadened pyridine peaks were observed at 7.15, 7.62, and 8.57 ppm, and these resonances did not shift upon addition of free pyridine. A broad singlet was observed at 2.12 ppm for the methyl groups of the *N*-aryl substituents on the pada²⁻ ligand, while the neighboring ortho aryl protons were broadened into the baseline of the spectrum.

To examine the kinetics of pyridine exchange, CDCl₃ solutions of **6** and two equivalents of free pyridine were monitored by variable-temperature ¹H NMR spectroscopy. Representative portions of the ¹H NMR spectra are shown in Figure 4. At 318 K, three sharp resonances are observed for pyridine protons at 8.58, 7.62, and 7.16 ppm. These resonances integrated to four equivalents of pyridine per titanium center, consistent with fast exchange between free and coordinated pyridine molecules. Upon cooling, these three resonances broaden and split into six resonances. At 219 K, six sharp resonances are observed for the pyridine protons, corresponding to two different pyridine environments. A doublet at 8.45 ppm (³*J*_{HH} = 4.9 Hz), a triplet at 7.60 ppm (³*J*_{HH} = 7.6 Hz), and an apparent triplet at 7.08 ppm can be assigned to pyridine coordinated to the titanium center, whereas the resonances at 8.65, 7.72, and 7.34 ppm correspond to free pyridine in solution. A one-to-one integration ratio for the coordinated and free pyridine signals suggests that the ground-state titanium species in solution is the five-coordinate complex observed in the solid state. Though the free and coordinated pyridine resonances overlap with the many other aryl resonances for **6**, crude

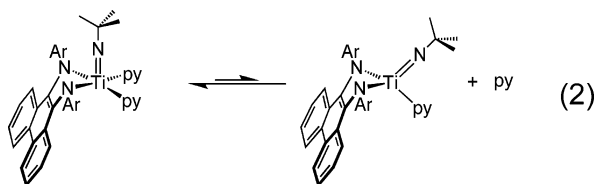
(89) Shi, Y.; Cao, C.; Odom, A. L. *Inorg. Chem.* **2004**, *43*, 275–281.

(90) Cundari, T. R. *J. Am. Chem. Soc.* **1992**, *114*, 7879–7888.

Scheme 4



estimates for the exchange rate constants could be obtained between 219 and 308 K; the activation parameters from an Eyring plot (see Supporting Information) are $\Delta H^\ddagger = 18 \pm 2$ kcal mol⁻¹ and $\Delta S^\ddagger = 19 \pm 7$ eu. The positive entropy value is indicative of dissociative ligand exchange to give a four-coordinate titanium imido intermediate, as shown in eq 2. This mechanistic assignment is further supported by concentration-dependence rate studies at 298 K, which gave an observed rate law that was independent of pyridine concentration. Furthermore, the activation parameters measured for **6** correspond well to those measured for dissociation of one pyridine from [PhC(NSiMe₃)₂]₂TiCl[=N(2,6-C₆H₃Me₂)](py)₂ to afford the five-coordinate monopyridine complex [PhC(NSiMe₃)₂]₂TiCl[=N(2,6-C₆H₃Me₂)](py).⁹¹



Reactivity of Titanium Imido Complex 6. Transimination reactivity has been observed between imido complex **6** and derivatives of aniline. As shown in Scheme 4, **6** reacts with 2,6-dimethylaniline in dichloromethane to afford the aryl imido complex (pada)Ti[=N(2,6-C₆H₃Me₂)](py)₂ (**7**) in 82% yield. This type of reaction, which is driven by the greater basicity of the alkylamine compared to the aniline, is well preceded for Group IV metals.^{39,54,59,85} Conversion to **7** can be monitored by ¹H NMR spectroscopy. While free 2,6-dimethylaniline dissolved in benzene-*d*₆ has a methyl signal at 1.88 ppm, the titanium–imido multiple-bond linkage induces a downfield shift of this methyl resonance to 2.40 ppm in **7**. This shift can be attributed to decreased shielding of the methyl protons brought about by strong N(π) \rightarrow Ti(d) lone pair donation, which is indicative of formation of the new Ti–N multiple bond.⁹¹ Other ¹H NMR features for **7** were strikingly similar to the parent complex **6**. Notably, the phenanthrene backbone resonances of **7** were observed at the same chemical shift values as for **6**. Three exchange-broadened pyridine peaks, observed at 6.24, 6.68, and 8.48 ppm, integrate to two pyridine ligands per

titanium center. Addition of free pyridine confirms that fast, dissociative pyridine exchange occurs on the NMR time scale. The strong similarity between the ¹H NMR features of **6** and **7** suggest an analogous coordination environment around the titanium arylimido fragment.

The well-known metathesis reactivity of Group IV imido complexes prompted an investigation of the reactivity of **6** with aldehydes, ketones, and imines (Scheme 4). The imine metathesis reaction has been used to convert aldehydes and ketones into aldimines and ketimines, respectively, via a [2+2] cycloaddition.⁹² Benzaldehyde reacted rapidly with **6** at room temperature in C₆D₆ to afford *N*-*tert*-butylphenylimine, as determined by GC-MS (*m/z* 161.20), which also showed complete consumption of the benzaldehyde substrate. When the reaction was followed by ¹H NMR spectroscopy, complete conversion was achieved in 3 h and a single (pada)titanium complex was observed. While this complex could not be isolated from the organic product, based on NMR data and literature precedent, it seems likely to be a bridging oxo complex, [(pada)Ti(py)(μ -O)]₂, though we cannot rule out a monomeric form analogous to **6**.

Preliminary studies suggest that complex **6** is unreactive with ketone and imine substrates but instead decomposes to form a dimeric complex. For example, a mixture of **6** and benzophenone in benzene-*d*₆ did not react at room temperature. Upon heating the solution to 80 °C, new ¹H NMR resonances appeared at the expense of the resonances for **6**; however, no change was observed for the benzophenone substrate. The transformation went to completion over 4 h. Similar behavior was observed when benzene-*d*₆ solutions of **6** were heated to 80 °C in the presence of *N*-2,6-dimethylphenylimine or in the absence of substrate. In these reactions, simple thermolysis of **6** leads to formation of a new titanium complex assigned as [(pada)Ti(py)(μ -N^{*t*}Bu)]₂ (**8**), shown in Scheme 4. The room-temperature ¹H NMR spectrum of **8** showed a new ^{*t*}Bu peak shifted upfield to 0.57 ppm, consistent with formation of a bridging imido ligand. Integration of the ¹H NMR spectrum gave a 1:1:1 ratio for the imido, pada, and pyridine ligands, suggesting that pyridine loss from **6** leads to formation of **8**. A molar mass determination for **8** gave 1300 \pm 180 g mol⁻¹, which is in reasonable agreement with the expected value of 1225.30 g mol⁻¹ for the formulation of **8**.⁹³ APCI mass spectrometry gave a *m/z* = 1067.5 for **8**, consistent with the [(pada)Ti(μ -N^{*t*}Bu)]₂core of **8** formed upon loss of the coordinated pyridine molecules during vaporization in the spectrometer.

Conclusion

The *N,N'*-bis(3,5-dimethylphenyl)phenanthrene-9,10-diamide ligand provided a framework for the synthesis of thermally stable and isolable titanium complexes with Ti–C, Ti–N, and Ti=N bonds. The relatively unhindered 3,5-dimethylphenyl substituents afforded four-, five-, and six-coordinate complexes. Preparation of titanium imido complex **6** via organometallic intermediates **4**, **5a**, and **5b**, respectively, is noteworthy because it involves a C–H bond 1,2-elimination. This process is related to the reversible C–H bond activation sequence reported for coordinatively unsaturated titanium imido complexes.^{28,94–96} In order to realize such C–H bond activation reactivity, the imido

(92) Lee, S. Y.; Bergman, R. G. *J. Am. Chem. Soc.* **1996**, *118*, 6396–6406.

(93) Burger, B. J.; Bercaw, J. E. In *Vacuum Line Techniques for Handling Air-Sensitive Organometallic Compounds*; Wayda, A. L., Darensbourg, M. Y., Eds.; Experimental Organometallic Chemistry; American Chemical Society: Washington, DC, 1987; pp 79–98.

(91) Stewart, P. J.; Blake, A. J.; Mountford, P. *Inorg. Chem.* **1997**, *36*, 3616–3622.

functionality must be generated on a low-coordinate metal center. Pyridine dissociation from **5a** and **5b** generates a four-coordinate species in benzene solution, and this species reacts with benzaldehyde. Unsaturated substrates with sterically demanding substituents, however, do not react with the (pada)-Ti(=NR)(py) fragment, and instead, dimerization appears to be the favored reaction path. This dimerization path also circumvents C–H bond reactivity, so future work will focus on phenanthrenediamide ligands with more sterically demanding substituents to block dimerization of low-coordinate imido species.

Experimental Section

General Procedures. The complexes described below are air and moisture sensitive, necessitating that manipulations be carried out under an inert atmosphere of argon or nitrogen gas using standard Schlenk, vacuum-line, and glovebox techniques. Hydrocarbon solvents were sparged with nitrogen and then deoxygenated and dried by passage through Q5 and activated alumina columns, respectively. Etheral and halogenated solvents were sparged with nitrogen and then dried by passage through two activated alumina columns. To test for effective oxygen and water removal, non-chlorinated solvents were treated with a few drops of a purple solution of sodium benzophenone ketyl in THF. Benzil, 3,5-dimethylaniline, potassium, and MeLi were purchased from Alfa Aesar and used as received. TiCl₄, LiN(SiMe₃)₂, and PhCH₂MgCl were purchased from Aldrich and used as received. Graphite was heated under dynamic vacuum overnight, pyridine was dried over sodium benzophenone and vacuum distilled, and ^tBuNH₂ and 2,6-dimethylaniline were dried over refluxing CaH₂ and distilled under argon. PhLi was prepared according to literature procedures⁹⁷ and used as a solid. Elemental analyses were performed by Desert Analytics. In most cases, satisfactory analyses were obtained; however, in the case of complexes **6** and **8**, low values for C and N were repeatedly obtained despite clean ¹H NMR spectra (see Supporting Information).

Physical Measurements. NMR spectra were collected on Bruker Avance 400 and 500 MHz spectrometers in dry, degassed benzene-*d*₆, chloroform-*d*₁, or THF-*d*₈. ¹H NMR spectra were referenced to TMS using the residual proteo impurities of the solvent; ¹³C NMR spectra were referenced to TMS using the natural abundance ¹³C impurities of the solvent. All chemical shifts are reported using the standard notation in parts per million; positive chemical shifts are to a higher frequency from the given reference. Infrared spectra were recorded as KBr pellets with a Perkin-Elmer Spectrum One FTIR spectrophotometer. Electronic absorption spectra were recorded with a Perkin-Elmer Lambda 800 UV/vis spectrophotometer.

Preparation of Bis(arylimino)bibenzyl. In a 3-neck round-bottom flask fitted with a reflux condenser, benzil (23.97 g, 114.0 mmol, 1 equiv) was dissolved in 300 mL of dry toluene under argon. 3,5-Dimethylaniline (48.36 g, 399.1 mmol, 3.5 equiv), 3 Å sieves, and 15 drops of HCl were then added to the round-bottom flask, and the mixture was heated to reflux for 48 h. After cooling to room temperature the sieves were removed by filtration and the toluene was removed under reduced pressure to yield a yellow, oily solid, which was dissolved in 200 mL of MeOH and stirred for 2 h. The product, bis(arylimino)bibenzyl, precipitated as a bright yellow solid that was collected by filtration and dried in vacuo (37.1 g, 78% yield). ¹H NMR (CDCl₃, 500 MHz) δ/ppm: 2.10 (s, 12H,

CH₃), 6.17 (s, 4H, *o*-CH), 6.65 (s, 2H, *p*-CH), 7.38–7.46 (m, 6H, Ar–H), 7.88 (d, 4H, *o*-Ar–H, ³J_{HH} = 7). ¹³C NMR (CDCl₃, 125.7 MHz) δ/ppm: 21.30 (CH₃), 118.31 (aryl-C), 126.47 (aryl-C), 128.37 (aryl-C), 128.73 (aryl-C), 131.12 (aryl-C), 137.81 (aryl-C), 137.92 (aryl-C), 149.38 (aryl-C–N), 164.10 (C=N). GC-MS *m/z* (% relative intensity, ion): 416 (99, M), 339 (10, M – C₆H₅), 207 (85, M – C₆H₅ – CNC₈H₉).

Preparation of padaH₂. Freshly cut potassium metal (5.599 g, 143.2 mmol, 6 equiv) and graphite (13.93 g, 116.0 mmol, 48 equiv) were combined in a 500 mL Schlenk flask. The flask was evacuated and heated gently to form KC₈ as a bronze solid. The flask was filled with argon gas, and THF (200 mL) was added to the KC₈ by cannula transfer. The KC₈ slurry was cooled in an ice–water bath, and a solution of bis(arylimino)bibenzyl (10.12 g, 24.05 mmol, 1 equiv) in 100 mL of THF was added by cannula transfer, resulting in an immediate color change to dark maroon. The reaction was stirred under argon for 12 h, at which time it was cooled again in an ice–water bath. The reaction was quenched by dropwise addition of 35 mL of MeOH. Upon warming to room temperature, the solid byproducts were removed by suction filtration and washed with 100 mL of diethyl ether. The golden-yellow organic phases were combined and extracted with 150 mL of water containing 10 g of NH₄Cl and then dried over MgSO₄. Solvent removal yielded an off-white bubbly solid. This residue was stirred with 20 mL of MeCN for 2 h at which time the product precipitated as a white solid (7.8 g, 78% yield). ¹H NMR (C₆D₆, 500 MHz) δ/ppm: 1.97 (s, 12H, CH₃), 5.51 (s, 2H, NH), 6.23 (s, 4H, *o*-Ar–H), 6.39 (s, 2H, *p*-Ar–H), 7.31 (dd, 2H, Ar–H), 7.38 (dd, 2H, Ar–H), 8.20 (d, 2H, Ar–H, ³J_{HH} = 8), 8.52 (d, 2H, Ar–H, ³J_{HH} = 8). ¹³C NMR (125.7 MHz) δ/ppm: 21.0 (C–CH₃), 113.2 (aryl-C), 121.5 (aryl-C), 123.0 (aryl-C), 125.4 (aryl-C), 126.2 (aryl-C), 126.8 (aryl-C), 130.1 (aryl-C), 130.5 (aryl-C), 131.4 (aryl-C), 138.7 (CN), 146.9 (CN).

Preparation of (pada)TiCl₂(py)₂ (1**).** In a nitrogen-filled glovebox, padaH₂ (2.83 g, 6.81 mmol, 1 equiv) was dissolved in dichloromethane (40 mL), and the solution was frozen in a liquid nitrogen cold well. In a separate vial, TiCl₄ (1.29 g, 6.81 mmol, 1 equiv) was dissolved in dichloromethane (15 mL), and the solution was frozen in a liquid nitrogen cold well. Both solutions were thawed, and the TiCl₄ solution was added to the solution containing padaH₂, resulting in an immediate color change to dark brown. ^tBuNH₂ (1.24 g, 17.0 mmol, 2.5 equiv) was added, and the reaction mixture was stirred while being warmed to box temperature (25.5 °C) for 2 h. Pyridine (2.47 g, 312 mmol, 4.5 equiv) was then added, and the reaction mixture was stirred for an additional 12 h. The reaction mixture was filtered to remove ^tBuNH₃Cl, and the dichloromethane was removed in vacuo to provide **1**, which was pure by ¹H NMR spectroscopy (4.5 g, 96% yield). Dark brownish black, X-ray quality crystals were grown by dissolving the product in dichloromethane and layering with pentane. Anal. Calcd for C₄₀H₃₆N₄Cl₂Ti·0.75CH₂Cl₂: C, 64.81; H, 5.00; N, 7.42. Found: C, 64.91; H, 5.42; N, 7.08. IR (KBr) ν /cm⁻¹: 699, 765, 832, 1038, 1207, 1312, 1441, 1600, 2914. UV/vis (CH₂Cl₂) λ_{max}/nm (ε/M⁻¹ cm⁻¹): 320 (13 717). ¹H NMR (CDCl₃, 500 MHz, 275 K) δ/ppm: 2.03 (s, 12H, CH₃), 6.43 (s, 2H, *p*-Ar–H), 6.57 (t, 4H, *m*-py–H), 7.05 (br, *o*-Ar–H), 7.21 (dd, 2H, Ar–H), 7.25 (t, 2H, *p*-py–H), 7.46 (dd, 2H, Ar–H), 7.73 (d, 2H, Ar–H, ³J_{HH} = 8), 8.29 (m, 6H, Ar–H, *o*-py–H). ¹³C NMR (125.7 MHz) δ/ppm: 21.4 (C–CH₃), 113.1 (NC–CH), 116.5 (CH₃C–CH), 121.4 (aryl-C), 122.5 (*m*-py–CH), 123.4 (aryl-C), 125.1 (aryl-C), 126.8 (aryl-C), 127.8 (aryl-C), 128.4 (*p*-py–CH), 137.7 (CN), 138.1 (C–CH₃), 149.9 (*o*-py–CH), 153.3 ((CH)₂–C–N).

Preparation of (pada)TiCl[N(SiMe₃)₂] (2**).** In a nitrogen-filled glovebox, **1** (0.24 g, 0.35 mmol, 1 equiv) was dissolved in diethyl ether (18 mL), and solid (Me₃Si)₂NLi (0.06 g, 0.35 mmol, 1 equiv) was added to the reaction mixture. After 4 h, the solution was filtered and the solvent removed in vacuo to afford **2** as a dark red

(94) Latesky, S. L.; McMullen, A. K.; Rothwell, I. P.; Huffman, J. C. *J. Am. Chem. Soc.* **1985**, *107*, 5981–5987.

(95) Bennett, J. L.; Wolczanski, P. T. *J. Am. Chem. Soc.* **1997**, *119*, 10696–10719.

(96) Cundari, T. R.; Klinckman, T. R.; Wolczanski, P. T. *J. Am. Chem. Soc.* **2002**, *124*, 1481–1487.

(97) Wehman, E.; Jastrzebski, J. T. B. H.; Ernsting, J.; Grove, D. M.; van Koten, G. J. *Organomet. Chem.* **1988**, *353*, 133–143.

solid (0.22 g, 96% yield). Anal. Calcd for $C_{36}H_{44}N_3ClSi_2Ti$: C, 65.69; H, 6.74; N, 6.38. Found: C, 65.97; H, 6.81; N, 6.21. IR (KBr) ν/cm^{-1} : 762, 843, 925, 1040, 1174, 1249, 1327, 1447, 1599, 2955, 3366. UV/vis (Et₂O) λ_{max}/nm ($\epsilon/M^{-1} cm^{-1}$): 413 (3839). ¹H NMR (C₆D₆, 500 MHz, 338 K) δ/ppm : 0.30 (br s, 18H, Si(CH₃)₃), 2.10 (br s, 12H, CH₃), 6.54 (s, 2H, *p*-Ar-H), 7.03 (dd, 2H, Ar-H), 7.24 (dd, 2H, Ar-H), 8.0 (d, 2H, Ar-H, ³*J*_{HH} = 5.5), 8.34 (d, 2H, Ar-H, ³*J*_{HH} = 8). ¹³C NMR (125.7 MHz) δ/ppm : 4.91 (Si-(CH₃)₃), 21.02 (CH₃), 117.43 (aryl-C), 123.15 (aryl-C), 123.70 (aryl-C), 126.04 (aryl-C), 126.16 (aryl-C), 126.89 (aryl-C), 133.36 (aryl-C-N), 138.80 (aryl-C), 151.56 (aryl-C).

Preparation of (pada)TiMe[N(SiMe₃)₂] (3a). In a nitrogen-filled glovebox, **2** (0.14 g, 0.21 mmol, 1 equiv) was dissolved in diethyl ether (10 mL), and the solution was frozen in a liquid nitrogen cold well. The solution was thawed, and MeLi (1.4 M, 0.15 mL, 0.22 mmol, 1 equiv) was added dropwise. The solution was allowed to warm to glovebox temperature with stirring for 3 h. The solution was filtered, and the solvent was removed in vacuo to afford **3a** as a reddish orange solid (0.13 g, 94% yield). Anal. Calcd for $C_{37}H_{47}N_3Si_2Ti$: C, 69.67; H, 7.43; N, 6.59. Found: C, 69.99; H, 6.69; N, 6.49. IR (KBr) ν/cm^{-1} : 762, 843, 925, 1040, 1174, 1249, 1327, 1447, 1599, 2955, 3366. UV/vis (toluene) λ_{max}/nm ($\epsilon/M^{-1} cm^{-1}$): 322 (15 079). ¹H NMR (C₆D₆, 500 MHz) δ/ppm : 0.25 (br s, 18H, Si(CH₃)₃), 0.44 (s, 3H, Ti-CH₃), 2.10 (br s, 12H, CH₃), 6.53 (s, 2H, *p*-Ar-H), 7.10 (dd, 2H, Ar-H), 7.28 (dd, 2H, Ar-H), 8.17 (d, 2H, Ar-H, ³*J*_{HH} = 8.5), 8.44 (d, 2H, Ar-H, ³*J*_{HH} = 8.5). ¹³C NMR (125.7 MHz) δ/ppm : 4.56 (Si-(CH₃)₃), 21.10 (C-CH₃), 23.53 (Ti-CH₃), 120.78 (aryl-C), 123.22 (aryl-C), 123.65 (aryl-C), 125.14 (aryl-C), 126.08 (aryl-C), 126.43 (aryl-C), 127.04 (aryl-C), 129.20 (aryl-C), 133.36 (aryl-C), 138.71 (aryl-C), 151.35 (aryl-CN).

Preparation of (pada)Ti(CH₂Ph)[N(SiMe₃)₂] (3b). Complex **3b** was prepared similarly to **3a** from PhCH₂MgCl (1 M, 0.418 mL, 0.418 mmol, 1 equiv) and **2** (0.2746 g, 0.417 mmol, 1 equiv) to give the product as a reddish orange solid (0.2173 g, 73% yield). Anal. Calcd for $C_{43}H_{51}N_3Ti$: C, 72.34; H, 7.20; N, 5.89. Found: C, 72.24; H, 6.87; N, 5.97. IR (KBr) ν/cm^{-1} : 688, 843, 1029, 1261, 1324, 1448, 1594, 2960. UV/vis (toluene) λ_{max}/nm ($\epsilon/M^{-1} cm^{-1}$): 329 (18 322). ¹H NMR (C₆D₆, 500 MHz, 340K) δ/ppm : 0.24 (br s, 18H, Si(CH₃)₃), 2.09 (s, 12H, CH₃), 2.35 (s, 2H, CH₂), 6.10 (t, 1H, *p*-CH), 6.21–6.23 (m, 4H, PhCH₂), 6.55 (s, 2H, *p*-Ar-H), 6.85 (s, 4H, *o*-Ar-H), 7.05 (dd, 2H, Ar-H), 7.29 (dd, 2H, Ar-H), 7.77 (d, 2H, Ar-H), 8.40 (d, 2H, Ar-H). ¹³C NMR (125.7 MHz) δ/ppm : 5.11 (Si-(CH₃)₃), 21.43 (CH₃), 120.80 (aryl-C), 121.53 (aryl-C), 123.69 (aryl-C), 124.73 (aryl-C), 125.58 (aryl-C), 125.78 (aryl-C), 126.29 (aryl-C), 126.90 (aryl-C), 127.41 (aryl-C), 129.15 (aryl-C), 133.83 (aryl-C), 138.94 (aryl-C), 151.51 (aryl-C).

Preparation of (pada)TiPh[N(SiMe₃)₂] (3c). Complex **3c** was prepared similarly to **3a** from PhLi (0.067 g, 0.797 mmol, 1 equiv) and **2** (0.5025 g, 0.763 mmol, 1 equiv) to give the product as a reddish orange solid (0.5088 g, 95% yield). Anal. Calcd for $C_{42}H_{49}N_3Ti$: C, 72.07; H, 7.06; N, 6.00. Found: C, 71.88; H, 7.17; N, 5.70. IR (KBr) ν/cm^{-1} : 763, 840, 1190, 1249, 1466, 1600, 2955, 3372. UV/vis (toluene) λ_{max}/nm ($\epsilon/M^{-1} cm^{-1}$): 320 (15 866). ¹H NMR (THF-*d*₈, 500 MHz) δ/ppm : 0.00 (s, 18H, Si(CH₃)₃), 2.18 (br s, 12H, Me), 6.49 (br m, 2H, *o*-Ph-CH), 6.62 (s, 2H, *p*-Ar-CH), 7.15 (dd, 2H, Ar-H), 7.20 (br m, 3H, Ph-H), 7.38 (dd, 2H, Ar-H), 7.63 (d, 2H, Ar-H, ³*J*_{HH} = 8), 8.52 (d, 2H, Ar-H, ³*J*_{HH} = 8). ¹³C NMR (C₆D₆, 125.7 MHz) δ/ppm : 4.60 (Si-(CH₃)₃), 21.17 (C-CH₃), 120.37 (aryl-C), 123.59 (aryl-C), 125.85 (aryl-C), 126.03 (aryl-C), 126.29 (aryl-C), 126.86 (aryl-C), 127.16 (aryl-C), 129.19 (aryl-C), 130.24 (aryl-C), 133.15 (aryl-C), 138.87 (aryl-C), 151.69 (aryl-C).

Preparation of (pada)Ti(CH₂Ph)₂(py) (4). In a nitrogen-filled glovebox, **1** (0.2133 g, 0.308 mmol, 1 equiv) was dissolved in diethyl ether (15 mL), and the solution was frozen in a liquid

nitrogen cold well. In a separate vial, a 1 M diethyl ether solution of PhCH₂MgCl (0.620 mL, 0.620 mmol, 2 equiv) was frozen in a liquid nitrogen cold well. Both solutions were allowed to thaw, and the PhCH₂MgCl solution was added dropwise to the cold solution of **1**. The reaction was stirred for 2 h at -35 °C, at which time the solution became medium red with an off-white precipitate. The solid was removed by filtration, and the solvent was removed in vacuo to afford **4** as a medium red solid (0.1773 g, 89% yield). ¹H NMR (C₆D₆, 500 MHz) δ/ppm : 1.93 (s, 4H, CH₂), 1.96 (s, 12H, CH₃), 6.42 (s, 2H, *p*-Ar-H), 6.61 (d, 4H, *o*-Ar-H, ³*J*_{HH} = 7.5), 6.70–6.89 (m, 13H, CH₂Ph-H and py-H), 7.17 (dd, 2H, Ar-H), 7.25 (dd, 2H, Ar-H), 8.24 (d, 2H, Ar-H, ³*J*_{HH} = 8), 8.43 (d, 2H, Ar-H, ³*J*_{HH} = 8.5), 8.67 (br, 2H, *o*-py-H).

Preparation of (pada)Ti(=N^tBu)(py)₂ (6). In a nitrogen-filled glovebox, **1** (3.175 g, 4.59 mmol, 1 equiv) and solid PhLi (0.790 g, 9.40 mmol, 2 equiv) were loaded into a 500 mL Schlenk flask. The flask was removed from the glovebox and attached to a vacuum line. Under argon, diethyl ether (200 mL) was added by cannula transfer to the Schlenk flask, which was cooled in a dry ice acetone bath. The reaction mixture was stirred for 2 h at -40 °C, during which time it became dark brownish red. Dry, degassed ^tBuNH₂ (0.49 mL, 4.62 mmol, 1 equiv) and pyridine (0.23 mL, 2.31 mmol, 0.5 equiv) were added with a syringe to the cold solution. Stirring was maintained for an additional 2 h while the reaction mixture warmed to room temperature. The resulting medium red solution was transferred to an air-free filter frit by cannula. Filtration and solvent removal afforded **6** as a medium reddish orange solid (1.6832 g, 53% yield). Crystals suitable for X-ray diffraction were grown from a diethyl ether solution chilled to -35 °C. IR (KBr) ν/cm^{-1} : 765, 828, 1040, 1190, 1339, 1599, 2958. UV/vis (toluene) λ_{max}/nm ($\epsilon/M^{-1} cm^{-1}$): 337 (12 837). ¹H NMR (C₆D₆, 500 MHz) δ/ppm : 1.49 (s, 9H, ^tBu), 2.18 (br s, 12H, CH₃), 6.30 (br, 4H, *m*-py-H), 6.48 (s, 2H, *p*-Ar-H), 6.65 (br, 2H, *m*-py-H), 7.11 (dd, 2H, Ar-H), 7.28 (dd, 2H, Ar-H), 8.07 (d, 2H, Ar-H, ³*J*_{HH} = 8), 8.55 (br, 4H, *o*-py-H), 8.56 (d, 2H, Ar-H, ³*J*_{HH} = 8). ¹³C NMR (125.7 MHz) δ/ppm : 21.11 (C-(CH₃)₃), 21.51 (C-CH₃), 33.07 (C-(CH₃)₃), 119.92 (aryl-C), 123.30 (aryl-C), 123.42 (aryl-C), 124.39 (aryl-C), 125.45 (aryl-C), 125.81 (aryl-C), 126.66 (aryl-C), 130.83 (aryl-C), 130.96 (aryl-C), 137.15 (aryl-C), 149.78 (aryl-C), 154.74 (aryl-C).

Preparation of (pada)Ti(=N-2,6-C₆H₃Me₂)(py)₂ (7). In a nitrogen-filled glovebox, **6** (0.1523 g, 0.220 mmol, 1 equiv) was dissolved in 16 mL of dichloromethane. 2,6-Dimethylaniline (0.030 mL, 0.242 mmol, 1 equiv) was added to the solution, and the mixture was stirred for 12 h. The solvent was removed in vacuo, and the resulting red solid was washed with cold heptane to produce pure **7** (0.1360 g, 82% yield). Anal. Calcd for $C_{48}H_{45}N_5Ti$: C, 77.93; H, 6.13; N, 9.47. Found: C, 78.10; H, 6.30; N, 9.25. IR (KBr) ν/cm^{-1} : 696, 757, 848, 1067, 1219, 1296, 1443, 1485, 1604. UV/vis (toluene) λ_{max}/nm ($\epsilon/M^{-1} cm^{-1}$): 335 (6438). ¹H NMR (C₆D₆, 500 MHz) δ/ppm : 2.03 (br s, 12H, *m*-CH₃), 2.45 (s, 6H, *o*-CH₃), 6.29 (br, 4H, *m*-py-H), 6.43 (s, 2H, *p*-Ar-H), 6.67 (br, 2H, *p*-py-H), 6.76 (t, 1H, *p*-Ar-H), 7.05 (d, 2H, *m*-Ar-H, ³*J*_{HH} = 7.5), 7.12 (dd, 2H, Ar-H), 7.30 (dd, 2H, Ar-H), 8.01 (d, 2H, Ar-H, ³*J*_{HH} = 8.5), 8.53 (m, 6H, Ar-H, *o*-py-H). ¹³C NMR (125.7 MHz) δ/ppm : 19.62 (*o*-CH₃), 21.39 (*m*-CH₃), 118.70 (aryl-C), 120.74 (aryl-C), 123.41 (aryl-C), 123.82 (aryl-C), 124.59 (aryl-C), 124.93 (aryl-C), 125.60 (aryl-C), 127.20 (aryl-C), 127.26 (aryl-C), 130.72 (aryl-C), 131.26 (aryl-C), 131.82 (aryl-C), 137.60 (aryl-C), 149.97 (aryl-C), 153.95 (aryl-C), 160.44 (aryl-C).

Preparation of [(pada)Ti(py)(μ-N^tBu)]₂ (8). In a Strauss tube, 100 mg of **6** (0.14 mmol, 1 equiv) was dissolved in benzene, and the solution was heated to 60 °C for 4 h, at which time the solution became dark red. The volatiles were removed in vacuo to afford **8** as a dark red solid (0.08 g, 82% yield). IR (KBr) ν/cm^{-1} : 761, 829, 1039, 1336, 1448, 1598. ¹H NMR (C₆D₆, 500 MHz) δ/ppm : 0.56 (s, 9H, ^tBu), 1.81 (br s, 6H, Me), 2.45 (br s, 6H, Me), 6.41

Table 3. Crystal Data Collection and Refinement Parameters

	(pada)TiCl ₂ (py) ₂ (1)	(pada)TiCl[N(SiMe ₃) ₂] ₂ ·C ₆ H ₆ (2 ·C ₆ H ₆)	(pada)Ti(=N ^t Bu)(py) ₂ ·OEt ₂ (6 ·OEt ₂)
empirical formula	C ₄₁ H ₃₈ Cl ₄ N ₄ Ti	C ₄₂ H ₅₀ ClN ₃ Si ₂ Ti	C ₄₈ H ₅₅ N ₅ O ₂ Ti
fw	691.53	736.38	765.87
cryst syst	monoclinic	triclinic	monoclinic
space group	<i>C2/c</i>	<i>P1</i>	<i>P2₁/n</i>
<i>a</i> /Å	34.856(7)	11.3545(16)	13.634(5)
<i>b</i> /Å	13.879(3)	12.0530(18)	20.831(7)
<i>c</i> /Å	15.984(3)	16.572(2)	16.889(6)
α /deg	90	84.444(3)	90
β /deg	107.438(3)	72.678(3)	110.676(5)
γ /deg	90	69.857(2)	90
<i>V</i> /Å ³	7377(3)	2032.7(5)	4488(3)
<i>Z</i>	8	2	4
reflns collected	28 914	21 173	23 466
independent reflns	5750	8926	7053
<i>R</i> 1	0.1202	0.0367	0.0667
<i>wR</i> 2	0.2976	0.0887	0.1510

(br m, 2H, *m*-py-H), 6.53 (s, 2H, *p*-Ar-H), 7.22 (dd, 2H, Ar-H), 7.29 (dd, 2H, Ar-H), 8.42 (br m, 2H, *o*-py-H), 8.46 (m, 4H, Ar-H). ¹³C NMR (125.7 MHz) δ /ppm: 21.30 (C-(CH₃)₃), 31.84 (C-CH₃), 71.23 (C-(CH₃)₃), 114.61 (aryl-C), 120.44 (aryl-C), 121.68 (aryl-C), 123.59 (aryl-C), 124.43 (aryl-C), 126.16 (aryl-C), 126.29 (aryl-C), 130.04 (aryl-C), 132.44 (aryl-C), 138.87 (aryl-C), 151.33 (aryl-C).

General Details of X-ray Data Collection and Reduction.

X-ray diffraction data for **2**·C₆H₆ were collected on a Bruker CCD platform diffractometer equipped with a CCD detector. Measurements were carried out at 163 K using Mo K α (λ = 0.71073 Å) radiation, which was wavelength selected with a single-crystal graphite monochromator. The SMART⁹⁸ program package was used to determine unit-cell parameters and for data collection. The raw frame data were processed using SAINT⁹⁹ and SADABS¹⁰⁰ to yield the reflection data files. Subsequent calculations were carried out using the SHELXTL¹⁰¹ program suite. Analytical scattering factors for neutral atoms were used throughout the analyses.¹⁰² Thermal ellipsoid plots were generated using the XP program within the SHELXTL suite. Diffraction data for **2**·C₆H₆ are shown in Table 3.

(98) SMART, Version 5.1; Bruker Analytical X-Ray Systems, Inc.: Madison, WI, 1999.

(99) SAINT, Version 5.1; Bruker Analytical X-Ray Systems, Inc.: Madison, WI, 1999.

(100) Sheldrick, G. M. SADABS, Version 2.05; Bruker Analytical X-Ray Systems, Inc.: Madison, WI, 2001.

(101) Sheldrick, G. M. SHELXTL, Version 6.12; Bruker Analytical X-Ray Systems, Inc.: Madison, WI, 2001.

(102) *International Tables for X-Ray Crystallography*; Kluwer Academic Publishers: Dordrecht, 1992; Vol. C.

X-ray diffraction data for **1** and **6**·OEt₂ were collected on a Bruker D8 platform diffractometer equipped with an APEX CCD detector at UC San Diego. Measurements were carried out at 100 K using Mo K α (λ = 0.71073 Å) radiation, which was wavelength selected with a single-crystal graphite monochromator. The SMART⁹⁸ program package was used to determine unit-cell parameters and for data collection. The raw frame data were processed using SAINT⁹⁹ and SADABS¹⁰⁰ to yield the reflection data files. Subsequent calculations were carried out using the SHELXTL¹⁰¹ program suite. Analytical scattering factors for neutral atoms were used throughout the analyses.¹⁰² Thermal ellipsoid plots were generated using the XP program within the SHELXTL suite. In the case of **1**, poorly resolved solvent disorder was rendered using SQUEEZE;¹⁰³ all intensive properties contain the solvent contributions. Diffraction data for **1** and **6**·OEt₂ are shown in Table 3.

Acknowledgment. The authors thank Antonio G. DiPasquale (UCSD) for assisting in X-ray data collection of complexes **1** and **6**, Jim Boncella for helpful suggestions, and the University of California, Irvine, for financial support.

Supporting Information Available: Eyring analyses for **2** and **6**, packing diagram for **2**, and X-ray diffraction data for **1**, **2**, and **6** (as CIFs). This material is available free of charge via the Internet at <http://pubs.acs.org>.

OM0701219

(103) Sluis, P. V. D.; Spek, A. L. *Acta Crystallogr.* **1990**, A46, 194.